Liquid Crystals
Publication details, including instructions for authors and subscription information:
http://www.informaworld.com/smpp/title~content=t713926090

Smectic A and C materials with novel director tilt and layer thickness behaviour

Marc D. Radcliffe; Myles L. Brostrom; Kenneth A. Epstein; Aaron G. Rappaport; Britt N. Thomas; Renfan Shao; Noel A. Clark

To cite this Article Radcliffe, Marc D. , Brostrom, Myles L. , Epstein, Kenneth A. , Rappaport, Aaron G. , Thomas, Britt N. , Shao, Renfan and Clark, Noel A.(1999) 'Smectic A and C materials with novel director tilt and layer thickness behaviour', Liquid Crystals, 26: 6, 789 — 794

To link to this Article: DOI: 10.1080/026782999204471

URL: http://dx.doi.org/10.1080/026782999204471

LIQUID CRYSTALS, 1999, VOL. 26, NO. 6, 789–794

Smectic A and C materials with novel director tilt and layer thickness behaviour

MARC D. RADCLIFFE, MYLES L. BROSTROM, KENNETH A. EPSTEIN,
AARON G. RAPPAPORT†, BRITT N. THOMAS‡, RENFAN SHAO†
and NOEL A. CLARK*†

3M Company, St. Paul, MN 55144, USA
† Department of Physics, University of Colorado, Boulder, CO 80309, USA
‡ Department of Chemistry, University of Wyoming, Laramie,
WY 82071-3838, USA

(*Received 31 August 1998; accepted 22 October 1998*)

We report a smectic liquid crystal in which a tilt of the molecular orientation away from the layer normal in the Smectic C phase of up to 24° occurs with minimal layer contraction. This characteristic, accompanied by an exceptionally large underlying negative thermal layer expansion coefficient, enables the formation of chiral smectic electro-optical cells having nearly the ideal 'bookshelf' layer geometry, free from the complexities of the chevron layer structure produced by contraction.

1. Introduction

The Smectic A (SmA) phase is a one dimensional stacking of two dimensional fluid layers in which the molecular director, **n**, giving the mean molecular long axis, is along the layer normal, **z**. As the temperature, T, is lowered, many SmA phases pass, via a second order phase transition (at temperature T_{AC}), to the Smectic C (SmC) phase, in which **n** tilts relative to z. This tilt is marked by the rotation of the optic axis away from z, through an equilibrium angle $\Theta_{opt}(T)$. In most smectic materials, such as the mixture CS1013, shown in figure 1, this molecular tilt is accompanied by layer contraction, a decrease in the SmC layer spacing $d_C(T)$ given approximately by $d_C(T) \sim d(T_{AC}) \cos[\Theta_{opt}(T)]$, where $d(T_{AC})$ is the layer spacing at the SmA–SmC transition, as might be expected for rigid rod-like molecules. In thin planar-aligned cells of the type used to produce electro-optic effects when filled with chiral SmC material (surface stabilized ferroelectric liquid crystal (SSFLC) cells [1], and others [2]), the contraction leads to the formation of the 'chevron' layer structure [3, 4], in which the layers bend away from an idealized 'bookshelf' geometry normal to the cell plates. Accompanying chevron layer formation there is a collection of distinctive effects, including 'zig-zag' defect formation [4–7], reduction of the effective optic axis rotation during switching, and cell-midplane orientational stabilization [8, 5, 6]. The complications resulting from these effects have generated some interest in methods for obtaining planar SmC alignment in the ideal bookshelf geometry, in which the layers simply remain normal or near-normal to the cell plates [9].

One approach for generating bookshelf alignment is to reduce the layer contraction accompanying the SmA–SmC phase transition, maintaining the bookshelf alignment of the SmA phase into the SmC phase. In most LC materials the layer spacing increases upon cooling in the SmA phase, i.e. the layer expansivity α_L is negative [$\alpha_L \equiv 1/d(\mathrm{d}d/\mathrm{d}T) < 0$]. This behaviour, opposite in sign to the usual thermal expansion behaviour of solids, is probably a consequence of increased effective molecular length as the flexible molecular tails become more extended at lower T. When α_L is negative, the layers expand upon cooling in the SmA phase, remaining under compression and in the bookshelf structure, becoming chevron only when layer contraction commences in the SmC phase. In this case $\delta(T)$, the angle of layer inclination away from bookshelf in the chevron structure is given by $\delta(T) = \cos^{-1}[d_C(T)/d(T_{AC})]$, and is controlled by $\Delta d(T) \equiv d_C(T) - d(T_{AC})$; as shown in figure 1, the layer contraction relative to $d(T_{AC})$ has its maximum value at the SmA–SmC transition. Recently, Mochizuki and co-workers have obtained such 'quasi-bookshelf' layer alignment in SSFLC cells in a family of molecules with naphthalene cores which, although their layers contract immediately upon cooling into the SmC phase, have overall negative layer thermal expansivities sufficiently large in magnitude to enable the

---

*Author for correspondence.

Journal of Liquid Crystals ISSN 0267-8292 print/ISSN 1366-5855 online ©1999 Taylor & Francis Ltd
http://www.tandf.co.uk/JNLS/lct.htm
http://www.taylorandfrancis.com/JNLS/lct.htm

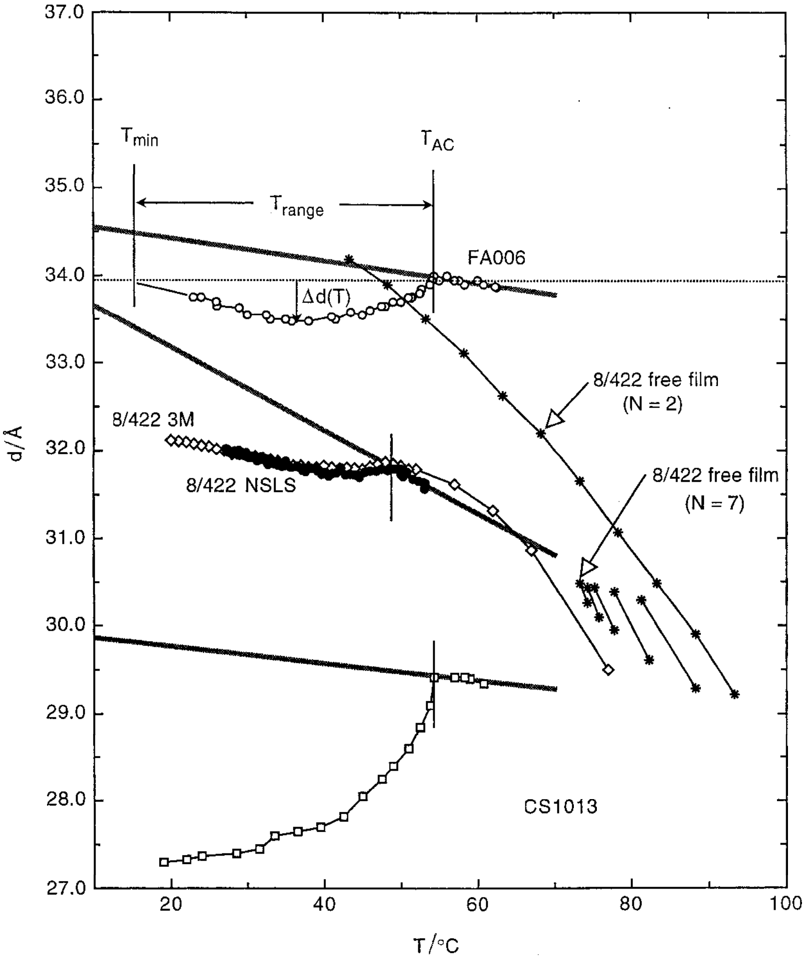

Figure 1. Smectic layer spacing $d(T)$ for 8/422, FA006, a mixture of naphthalene core molecules developed by Mochzuki and coworkers [10], and Chisso mixture CS1013 [10]. All three materials exhibit a second order SmA–SmC phase transition as indicated. For 8/422 data taken at both NSLS (●) and 3M (◇) are shown. Also shown are measurements from ref. [14] of 8/422 layer thickness in freely suspended films having $2 < N < 7$ layers. The solid grey lines are fits of $d_A(T) = d_0 + \alpha_L T$ to the SmA phase data, where α_L is the SmA layer expansion coefficient near the SmA–SmC phase transition. 8/422 has the largest $|\alpha_L|$ of the three and the smallest layer contraction upon cooling into the SmC phase. Both FA006 and 8/422 exhibit a minimum $d(T)$ in the SmC phase, with $d(T)$ increasing back to $d(T_{AC})$, the value at the SmA–SmC phase transition, as T is lowered to T_{min} in the SmC phase.

layer spacing to again recover its SmA–SmC transition value $d_C(T_{AC})$ at a temperature $T_{min} = T_{AC} - T_{range}$ below the SmA–SmC transition. This behaviour can be quantified by measuring $|\Delta d_{max}|$, the magnitude of the maximal layer contraction, and T_{range}, the width of the temperature range where $\Delta d < 0$ [10–12]. Figure 1 shows $d(T)$ for such a naphthalene mixture (FA006), indicating $\Delta d(T)$, T_{min}, and T_{range}. In order to be optimal, such quasibookshelf materials should combine minimal $|\Delta d_{max}|$ with maximum T_{range}, yielding nearly upright layers over a wide temperature range, while maintaining a useful optical tilt, i.e. $\Theta_{opt}(T)$ saturating at low T in the range $20° < \Theta_{opt}(T) < 25°$. Here we report X-ray $d(T)$ and optical Θ_{opt} data for the fluoroether-tail LC material '8/422', which exhibits desirable characteristics for quasibookshelf application. 8/422 is the compound 2-{4-[1,1-dihydro-2-(2-perfluorobutoxyperfluoroethoxy)-perfluoroethoxy]}phenyl-5-octylpyrimidine [13],

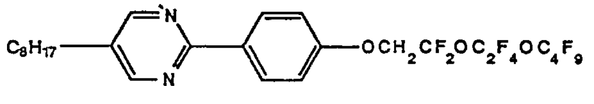

I 70°C SmA 49°C SmC – 8°C Cr

which has Isotropic (I), SmA, SmC, and Crystal (Cr) phases, as indicated.

2. Results

Two distinct sets of X-ray diffraction measurements of the layer spacing in the smectic phases of 8/422 were obtained, one on beamline X10-B of the National Synchrotron Light Source (NSLS), and one at 3M on a Kratky SAXS (Small Angle X-ray Scattering) system with resolution in wavevector $\delta q = 0.001$ Å^{-1}, using a Rigaku RU-200 Ni filtered CuK$_\alpha$ source and fitted with a Braun 5 cm linear position sensitive detector. The samples were unoriented, contained in quartz capillaries which were in turn mounted in a temperature controlled aluminum oven. The smectic layer spacing was $d \sim 32$ Å, corresponding to a Bragg wave vector $q_0 \sim$ Å^{-1}. At NSLS the incident X-ray wavelength was $\lambda = (0.97090 \pm 0.00005)$ Å, and resolution in wavevector of $\delta q = \pm 0.0001$ Å^{-1} enabled individual measurements of layer spacing $d = 2\pi/q_0$ to be obtained with an uncertainty of $\pm 0.005\%$. These two $d(T)$ data sets agreed to within experimental uncertainty at temperatures where they overlapped. The optical tilt of 8/422 was measured using 2 μm thick SSFLC cells by adding 1–5 wt % of a chiral dopant to make the SmC ferroelectric and by applying an electric field large enough to saturate the apparent rotation of the optic axis.

Figures 1 and 2 show the resulting $d(T)$ vs. T data for 8/422. Figure 1 displays the 8/422 data along with that of FA006 and CS1013 for comparison [10]. For each material the solid grey line gives $d_A(T) \equiv d_0 + \alpha_L T$, the SmA phase layer spacing, and its extrapolation obtained assuming linear thermal expansion and least squares fitting the SmA phase $d(T)$ data near the SmA–SmC transition. In CS1013, which has behaviour typical of most smectics with respect to $d(T)$, there is a rather low $|\alpha_L|$ in the SmA phase and d decreases abruptly upon entering the SmC phase at T_{AC}. By contrast 8/422 has an overall negative α_L of exceptionally large magnitude, especially at higher temperatures in the SmA phase and very little decrease of d in the SmC phase. The naphthalene core mixture FA006 has a temperature dependence of $d(T)$ intermediate between 8/422 and CS1013.

Figure 1 also shows the 8/422 layer spacing obtained by optical reflectivity measurements on freely suspended films [14]. These films are quantized in thickness, consisting of N smectic layers, and the film thickness is calculated from the reflectivity assuming an N-independent refractive index $n_0 = 1.45$ for 8/422 [14]. This assumption yields a significant layer contraction with increasing N, with the layer thickness for $N = 2$ nearly 2 Å larger than for the bulk. In plotting the data of reference [14] onto figure 1, n_0 was scaled to $n_0 = 1.462$ so that the film data extrapolate at large N to the bulk $d(T)$. The $d(T)$ of the films exhibit the large α_L of the bulk SmA phase at high T. For $N = 2$ this large α_L is apparent over the range 40°C $< T <$ 95°C, remarkably showing no hint of the decrease and sign change associated with the bulk SmA–SmC transition.

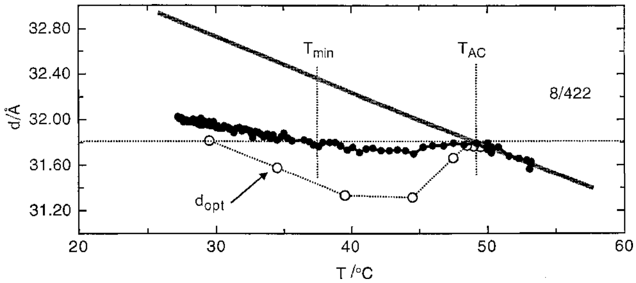

Figure 2. 8/422 $d(T)$ data (●) showing T_{AC} and T_{min}, $d_A(T) = a + \alpha_L T$ (solid grey line), and $d_{opt}(T) = d_A(T) - d_{core}\cos(\Theta_{opt})$ (○). $d_{opt}(T)$ is the layer spacing expected from subtraction of shrinkage due to the tilt of the molecular core through the optical tilt angle Θ_{opt} from the extrapolated SmA layer spacing.

The behaviour of the layer spacing and optical tilt can be characterized using the two ratios:

$$f \equiv \Theta_{Xray}(T)/\Theta_{opt}(T) \equiv \cos^{-1}(d_C(T)/d_A(T)]/\Theta_{opt}(T) \quad (1)$$

$$R \equiv \delta(T)/\Theta_{opt}(T) \equiv \cos^{-1}[d_C(T)/d(T_{AC})]/\Theta_{opt}(T). \quad (2)$$

Here $\Theta_{Xray}(T) = \cos^{-1}[d_C(T)/d_A(T)]$ is the 'X-ray tilt', the tilt of the molecules, assuming that they behave as rigid rods, necessary to give the layer shrinkage in the SmC phase relative to $d_A(T)$ extrapolated into the SmC phase; $\delta(T) = \cos^{-1}[d_C(T)/d(T_{AC})]$ is the chevron layer tilt angle, the layer inclination necessary to accommodate the shrinkage of the layers from their value at the SmA–SmC transition. Since α_L, the layer expansivity in the SmA phase, is negative, we will always have $f > R$. The ratio R can be considered a figure of merit for a material with respect to its performance in the SSFLC geometry, this approaching the idealized 'bookshelf' geometry as $R \to 0$.

8/422 exhibits atypical behaviour with respect to the temperature dependence of f and R. Figure 3 shows measurements of $\Theta_{opt}(T)$ vs. $\Delta T = T_{AC} - T$ for the three materials, along with their X-ray tilt $\Theta_{Xray}(T)$. CS1013 exhibits the typically observed relationship between $\Theta_{Xray}(T)$ and $\Theta_{opt}(T)$, in which $0.7 < f < 0.9$ ($f \approx 0.875$ for CS1013). By contrast, in 8/422, $\Theta_{opt}(T)$ is much larger than $\Theta_{Xray}(T)$, rising quickly with decreasing T and saturating at $\Theta_{opt} \sim 24° \sim 2\Theta_{Xray}$. Also indicated in figure 3 is the chevron layer tilt angle $\delta(T)$ (solid grey line). For CS1013 $\delta \sim \Theta_{Xray}$, increasing continuously with decreasing T, whereas it reaches a maximum and then decreases with T for FA006 and 8/422, returning to $\delta = 0$ at $T = T_{min}$. In 8/422, $\delta(T)$ remains quite small [$\delta(T) < 5°$] for $T_{AC} < T < T_{min}$, because of the small decrease in $d(T)$ upon entering the SmC phase. Because $R \ll 1$, SSFLC cells made with 8/422 have essentially the ideal bookshelf structure, optical characteristics, and bistability [1].

A variety of homologues of 8/422 have been synthesized and similarly tested. These experiments show that it is the incorporation of a fluoroether tail that tends to reduce R. In contrast to the naphthalene based materials, a particular core structure is not essential for small R. For example, analogues of 8/422 with phenyl benzoate cores exhibit $d(T)$ characteristics similar to those having the phenyl pyrimidine core and have similarly low values of R [13]. By contrast, replacement of the fluoroether tail with a fluoroalkyl tail gives the fluoroalkyl phenylpyrimidenes [15, 16]

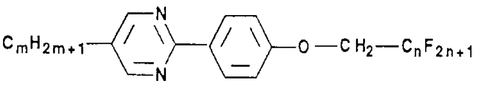

m/n series

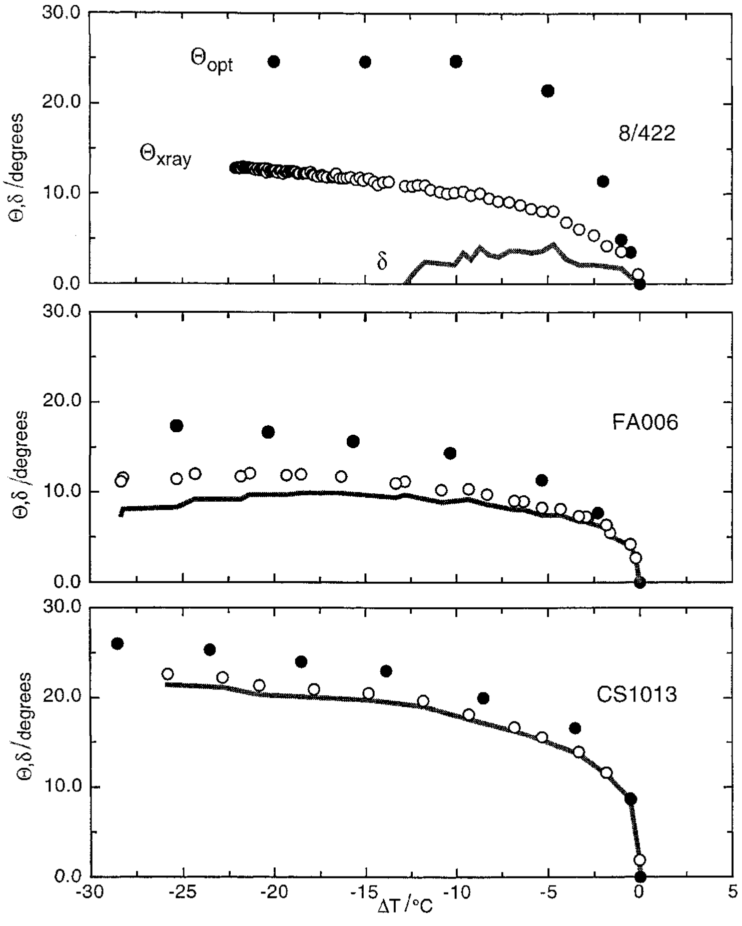

Figure 3. Optical tilt angles $\Theta_{\rm opt}$ (●) for 8/422, FA006, and CS1013 vs. $\Delta T = T_{\rm AC} - T$. $\Theta_{\rm opt}$ is determined by measuring saturation extinction orientation under applied field. Also plotted are $\Theta_{\rm Xray} = \cos^{-1}[d_{\rm C}(T)/d_{\rm A}(T)]$ (○), and the chevron layer inclination upon cooling, $\delta = \cos^{-1}[d_{\rm C}(T)/d(T_{\rm AC})]$ (solid grey line). 8/422 has a uniquely small value for the ratio $R = \delta/\Theta_{\rm opt}$.

which have a fundamentally different $d(T)$ behaviour, as shown in figure 4. Here we combine the $d(T)$ data of Rieker and Janulis [15] with optical tilt measurements to give $\Theta_{\rm opt}(T)$, $\Theta_{\rm Xray}(T)$, and δ. We find $f \approx 1$ and $R \approx 1$ for the m/n series, in sharp contrast to 8/422.

3. Discussion

The most interesting question about the $d(T)$ behaviour of 8/422 is how such a large SmC phase tilt angle can accompany such a small decrease in layer thickness. The simplest model of the relationship between $\Theta_{\rm opt}(T)$ and $d_{\rm C}(T)$ in the SmC phase is to visualize a hypothetical SmC phase which has rigid rod molecules with their optical axis along the rod axis and which tilt to produce the layer shrinkage upon entering the SmC phase. Ignoring the SmA layer expansivity we would expect to find $d_{\rm C}(T)/d_{\rm A}(T) = \cos[\Theta(T)]$, where $\Theta(T)$ is the tilt of the molecular axis, and therefore $\delta(T) = \Theta_{\rm Xray}(T) = \Theta_{\rm opt}(T) = \Theta(T)$; that is, we would find $f = R = 1$, as in the fluoroalkyl m/n series (figure 4). There are several ways in which this simple picture can break down to give f, $R < 1$, as described in the following sections.

3.1. *d(T) is controlled by the tilt of the core and tail segments of individual molecules. If $f < 1$, then the average molecular tilt is less than $\Theta_{opt}(T)$*

Since it is the core part of the molecule which generates the optical anisotropy, we expect the average tilt of the core part, $\Theta_{\rm core}(T)$, to be comparable to $\Theta_{\rm opt}(T)$, meaning that then $\Theta_{\rm tail}(T)$ must be less than $\Theta_{\rm opt}(T)$. Writing

$$d_{\rm C}(T) = d_{\rm core}\cos[\Theta_{\rm core}(T)] + d_{\rm tail}\cos[\Theta_{\rm tail}(T)] \quad (3)$$

where $d_{\rm core}$ and $d_{\rm tail}$ are the effective thicknesses of the core and tail regions in the SmA phase, respectively, and taking $\Theta_{\rm opt}(T) = \Theta_{\rm core}(T)$, we have

$$d_{\rm A}(T)\cos[f\Theta_{\rm opt}(T)] = d_{\rm core}\cos[\Theta_{\rm opt}(T)] + d_{\rm tail}\cos[\Theta_{\rm tail}(T)]. \quad (4)$$

This transcendental equation may be solved for $\Theta_{\rm tail}(T)$, which is smaller than $\Theta_{\rm core}(T) = \Theta_{\rm opt}(T)$ when $f < 1$. The extreme case, giving the *least* layer shrinkage, is to assume $\Theta_{\rm tail} = 0$, in which case from equation (3):

$$d_{\rm C}(T) = d_{\rm opt} \equiv d_{\rm core}\cos[\Theta_{\rm opt}(T)] + d_{\rm tail}. \quad (5)$$

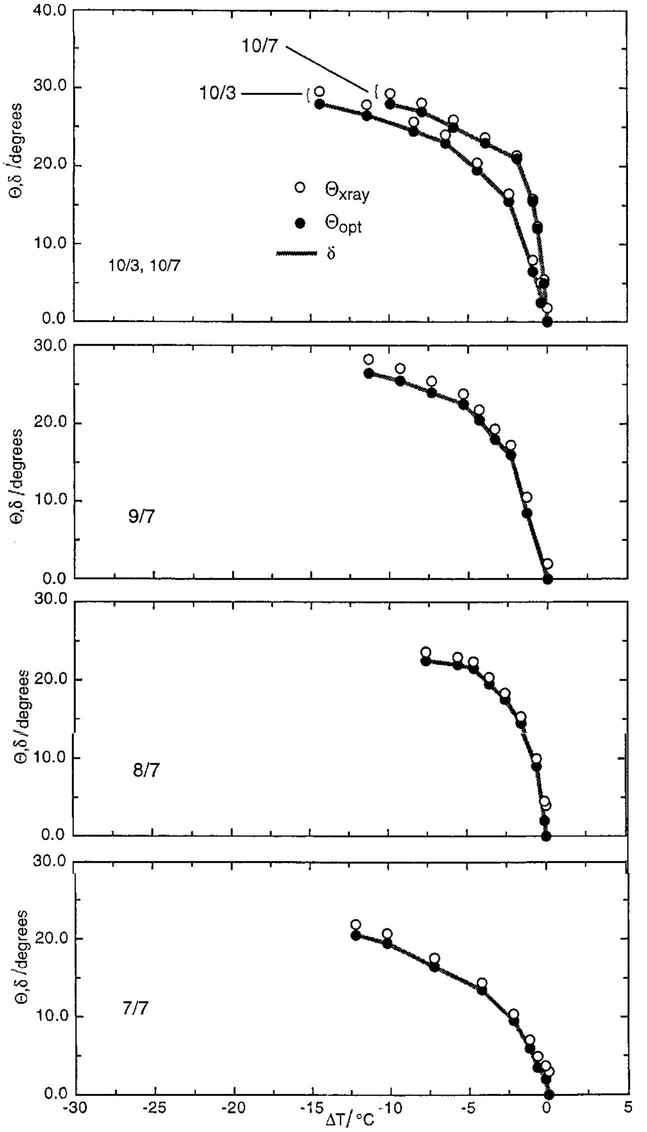

Figure 4. Optical tilt angles Θ_{opt} (●) for the *m*/*n* fluoroalkyl phenylpyrimidine series vs. $\Delta T = T_{AC} - T$. Θ_{opt} is determined by measuring saturation extinction orientation under applied field. Also plotted are $\Theta_{Xray} = \cos^{-1}[d_C(T)/d_A(T)]$ (○), and the chevron layer inclination upon cooling, $\delta = \cos^{-1}[d_C(T)/d(T_{AC})]$ (solid grey line), which give $f = R \approx 1$.

Figure 2 shows d_{opt} for 8/422, which drops significantly below the measured $d(T)$, except at the lowest temperatures in the SmC phase, where it approaches $d(T)$, being ~0.8 Å less than the extrapolated $d_A(T)$, comparable to the shrinkage due to the 9.8 Å long core of 8/422 tilted through 24°. However the big discrepancy at higher temperatures in the SmC phase indicates that core tilt gives a much larger layer shrinkage than is observed, i.e. simple core tilt cannot account for $d(T)$ in 8/422.

3.2. *The molecules are already tilted in the SmA phase*

The SmA phase may be a 'deVries' smectic A [17], in which the molecules are tilted on a cone of angle Θ_{DV}, but where the tilt order is short ranged, becoming long ranged at the SmA–SmC transition. The extreme case of tilt in the SmA phase has $\Theta_{DV} = \Theta_{opt\,sat} \approx 25°$, the saturation value of Θ_{opt} at low temperature, and, upon entering the SmC phase, the azimuthal ordering on the cone becomes more localized to a single orientation without layer contraction. In this case $d_C(T)/d_A(T) \approx 1$ and, therefore, $\Theta_{Xray}(T) \approx 0$ and $f, R \approx 0$. If $\Theta_{DV} < \Theta_{opt\,sat}$, there will be some layer contraction in the SmC phase as the azimuthal distribution on the cone becomes more localized, and $f, R > 0$. In the limit that $\Theta_{DV} = 0$, we have $f, R \approx 1$. With the deVries scenario, $\Delta n_A = n_{\parallel} - n_{\perp}$, the uniaxial birefringence in the SmA phase, is related to Δn_C (the birefringence in the SmC phase observed with the director parallel to the cell plates) by $\Delta n_A/\Delta n_C = \cos^2\Theta_{DC} - 0.5\sin^2\Theta_{DV}$. Where we have assumed that the azimuthal orientation on the cone is random in the SmA and confined to a single point in the SmC. The apparent Θ_{Xray} at low temperature, where $\Theta_C \sim \Theta_{Csat}$, will be given by $\Theta_{Xray} = \cos^{-1}[1 + \cos\Theta_A + \cos\Theta_C]$. Relative measurements of the optical anisotropy at $T = 50°C$ (SmA), 40°C (SmC), and 25°C (SmC) show that the Δn values at these three temperatures are in the ratio 1: 1.12: 1.20, an increase with decreasing T which is much larger than typically found in SmC phases [18]. Thus, at $T = 40°C$, the smectic C tilt angle is already saturated at $\Theta_{Csat} = 25°$ and $\Delta n_C\,(40)/\Delta n_A\,(50) = 0.89$, which is consistent with a $\Theta_A = 15.7°$. In this case the apparent Θ_{Xray} will be $\Theta_{Xray} = 19.3°$, somewhat larger that the observed Θ_{Xray}. At $T = 25°$, the SmC tilt angle is at $\Theta_{Csat} = 25°$ and $\Delta n_C\,(25)/\Delta n_A\,(50) = 0.83$, which is consistent with a $\Theta_A = 19.4°$. In this case the apparent Θ_{Xray} will be $\Theta_{Xray} = 15.4°$, comparable to the observed value. Thus, the comparison of layer spacing and birefringence at high and low temperature is consistent with the deVries picture. The possibility of a deVries smectic A will be probed more definitively using infrared dichroism.

3.3. *d(T) is influenced by molecular interdigitation and fluoroether tail flexibility*

Measurements on smectic phases of hybrid molecules having one hydrocarbon and one fluorocarbon chain (bulk smectic layer spacing vs. chain lengths [15, 16], and surface tension measurements in freely suspended films [19]) show that on average the adjacent molecules are packed *antiparallel* to one another, i.e. with each hydrocarbon tail tending to be surrounded by fluorocarbon tails and vice-versa. Furthermore, the absence of nematic phases in such materials indicates that the tendency for particular antiparallel positional correlation is quite strong. This situation favours the formation of smectic phases, in particular those having layer spacings which can differ substantially from the extended molecular length. For example, in the *m/n* series, the smectic layer spacing is independent of the hydrocarbon tail length, being determined a 'network' of associating cores and the fluoroalkyl tails [15, 16]. The fluoroalkyl tails are rigid and rod-like and the smectic layer spacing increments with increasing *n* directly as the change in the fluoroalkyl tail length.

The fluoroether tails are, by contrast, quite flexible, having a lower energy cost for rotational isomerization out of the minimum-energy, linear, all-*trans*-state than either the fluoroalkyl or alkyl tails. The corresponding chain fluctuations effectively foreshorten the fluoroether tails, and it is the reduction of these fluctuations with decreasing temperature which most likely generates the large negative α_L in the SmA phase of 8/422. The SmA layer expansion in 8/422 continues with decreasing temperature until the SmA–SmC transition, where the layer spacing, d_{AC}= 31.8 Å, has become comparable to the extended molecular length, 31.9 Å for 8/422 as determined from Alchemy III. Similar behaviour is found in other 8/422 homologues. The layer expansion is accompanied by a decreasing value of A, the area per molecule parallel to the layer plane, and an increased importance of enthalpic vs. entropic intermolecular interactions. Apparently the enthalpic interactions drive longitudinal relative displacement of the cores, an intrinsic requirement for SmC formation.

Comparison of the behaviour of the fluoroalkyl *m/n* series and 8/422 and its homologues shows that the balance of the rates of molecular extension and longitudinal relative core displacement with changing temperature is strongly dependent on the structural details of the fluorinated tails. In the case of the fluoroalkyl series, the SmC core tilt occurs with the molecules behaving essentially as rigid rods, with A increasing and d decreasing as $\cos \Theta_{\mathrm{opt}}$. In the plane normal to the molecular long axes, the area per molecule, A_N, is essentially independent of tilt. By contrast, in 8/422 the core tilt in the SmC phase occurs with essentially constant A and d, and, therefore A_N must decrease as the temperature is lowered from T_{AC} to $T_{\min}$. This decrease in area per molecule appears to be a consequence of the temperature dependence of the effective size of the fluoroether tail, determined by a combination of steric and entropic effects.

This work was carried out in part at the National Synchrotron Light Source, and supported in part by NSF Grant DMR 96-14061 and NSF MRSEC Grant 98-09555.

References

[1] Clark, N. A., and Lagerwall, S. T., 1980, *Appl. Phys. Lett.*, **36**, 899.

[2] Crawford, G., Geer, R. E., Naciri, J., Shashidhar, R., and Ratna, B. N., 1995, *Appl. Phys. Lett.*, **65**, 2937; Rappaport, A. G., Williams, P. A., Thomas, B. N., Clark, N. A., Blanca Ros, M., and Walba, D. M., 1995, *Appl. Phys. Lett.*, **67**, 362.

[3] Rieker, T. P., Clark, N. A., Smith, G. S., Parmar, D. S., Sirota, E. B., and Safinya, C. R., 1987, *Phys. Rev. Lett.*, **59**, 2658.

[4] Clark, N. A., and Rieker, T. P., 1988, *Phys. Rev. A: Rapid Commun.*, **37**, 1053.

[5] Clark, N. A., Rieker, T. P., and Maclennan, J. E., 1988, *Ferroelectrics*, **85**, 79.

[6] Rieker, T. P., and Clark, N. A., 1992, *Phase Transitions in Liquid Crystals*, edited by S. Martellucci (New York: Plenum), p. 287.

[7] Handschy, M. A., and Clark, N. A., 1984, *Ferroelectrics*, **59**, 69.

[8] Ouchi, Y., Takezoe, H., and Fukuda, A., 1987, *Jpn J. appl. Phys. I*, **26**, 1.

[9] Hartmann, W. J. A. M., and Luyckx-Smolders, A. M. M., 1970, *J. appl. Phys.*, **67**, 1253.

[10] Mochizuki, A., 1991, PhD thesis, Tokyo University of Agriculture and Technology.

[11] Mochizuki, A., Nakatsuka, M., Takanashi, Y., Ouchi, Y., Takezoe, H., and Fukuda, A., 1989, in *Proceedings of the 9th International Display Research Conference*, Kyoto, 1989 (SID, 1989), p. 30.

[12] Takanashi, Y., Ouchi, Y., Takezoe, H., Fukuda, A., Mochizuki, A., and Nakatsuka, M., 1990, *Jpn J. appl. Phys.*, **29**, L984.

[13] Epstein, K. A., Keyes, M. P., Radcliffe, M. D., and Snustad, D. C., 1995, US Patent No. 5 417 883.

[14] Mach, P., Johnson, P. M., Wedell, E. D., Lintgen, F., and Huang, C. C., 1997, *Europhys. Lett.*, **40**, 399.

[15] Rieker, T. P., and Janulis, E. P., 1994, *Liq. Cryst.*, **17**, 681.

[16] Rieker, T. P., and Janulis, E. P., 1995, *Phys. Rev. E.*, **52**, 2688.

[17] DeVries, A. J., 1977, *Mol. Cryst. liq. Cryst. Lett.*, **41**, 27.

[18] Lockhart, T. E., Allender, D. W., Gelerinter, E., and Johnson, D. L., 1979, *Phys. Rev. A*, **20**, 1655.

[19] Mach, P., Huang, C. C., and Nguyen, H. T., 1998, *Phys. Rev. Lett.*, **75**, 4047; Mach, P., Huang, C. C., Stoebe, T., Wedell, E. D., Nguyen, H. T., deJeu, W. H., Guittard, F., Naciri, J., Shashidhar, R., Jiang, I. M., Kao, F. J., and Liu, H., 1998, *Langmuir*, **14**, 4330.